31st Annual International Conference of the IEEE EMBS
Minneapolis, Minnesota, USA, September 2-6, 2009

Effect of a magnetic core in the receiver coil of a biomedical inductive power system

Furqan Noor, Maeve Duffy, *Member, IEEE*

Abstract—The design of an inductive power system is investigated in order to determine the relative benefits provided by the inclusion of a magnetic core in the receiver coil. Both transmitter and receiver coils are chosen to have dimensions similar to those used in many biomedical devices. It is found that while a magnetic core provides enhanced coupling, the operating frequency is limited by losses in the magnetic material. Consequently, the performance of air-core coils is shown to match that of coils with magnetic cores when operated at a higher frequency. Work is ongoing to consider the effects of other limitations imposed by biomedical environments.

I. Introduction

Inductive powering is widely used in biomedical devices, where the advantages of a wireless power link include reduced infection due to wire connections and the elimination of repeated surgery for replacement of batteries [1]. Several different inductive coil combinations have been considered for the transmitter and receiver sides, both with and without magnetic material [2–4]. The focus of this paper is on flat, wide transmitter coils and long, narrow receiver coils, where the receiver coil is implanted at least. The main objective is to determine the relative advantage of including magnetic material in the receiver coil in terms of the maximum power level that can be provided.

The geometry and size of the receiver are selected to be very small compared to the transmitter coil to simulate what is required in many biomedical implants [1], [3], [5]. Due to this size limitation, the range of magnetic materials available for use as receiver core materials is limited. Nonetheless, it is shown that the introduction of a demonstrator core material improves the power levels achievable with a given inductive power system. Circuit models are applied to determine the limit in power achieved in all cases, whereby it is found that self resonance is the limiting factor in the case of an air-coil, while loss properties of the core material limit power transfer in a coil with a core. Results are verified by measurements on a demonstrator test system. Work is ongoing to investigate other magnetic materials that may be applied with a view to increasing delivered power levels.

Manuscript received April 7, 2009. This work is supported by Enterprise Ireland and Brivant Ltd. under Grant IP/2007/0447.

M. Duffy is with the Power Electronics Research Centre, Department of Electrical & Electronic Engineering, National University of Ireland, Galway, IRELAND (e-mail: maeve.duffy@nuigalway.ie).

F. Noor is with the Bioelectronics Research Cluster, Department of Electrical & Electronic Engineering, National University of Ireland, Galway, IRELAND (e-mail: f.noor1@nuigalway.ie).

Components of the test system are described in section II, including the structure and materials of the transmitter and receiver coils. Equivalent circuit parameters are determined through analytic formulas and testing. The procedure for designing resonant circuits in which the inductive impedance of transmitter and receiver coils is compensated is described in section III, along with different methods for determining circuit Q-factors. Measurement results are presented for given inductive coils, both with and without magnetic material. The coils are fixed at an axial distance of 55 mm apart and the variation in power with frequency is investigated. Continuous power levels of up to 0.1 mW are demonstrated for a receiver coil with an outer diameter of 5 mm and a length of 10 mm.

II. Overview of Test System and Inductive Coils

A circuit diagram of the test system applied in both cases of air and magnetic cores is shown in Fig. 1. The function generator acts as a power supply feeding the transmitter coil through a parallel resonant tank, and a second resonant capacitor is connected across the receiver coil in parallel with a load resistor. In practice, power would be supplied from a battery through a Class E power amplifier [6], [7].

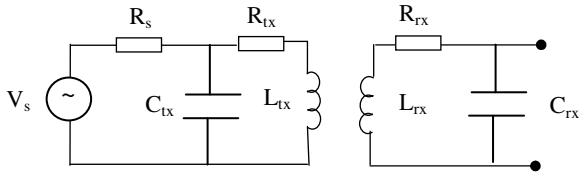

Fig. 1. Circuit diagram of inductive power test system

In order to be comparable with other inductive power systems for biomedical applications, a transmitter coil with outer diameter of 51 mm was wound with N_{tx} = 10 turns of wire having with a diameter, d_{wtx}, of 0.5 mm. A cross section of the coil is shown in Fig. 2. Values of resistance, R_{tx}, and inductance, L_{tx}, were predicted using the simple formulas:

$$R_{t/rx} = \frac{4N_{t/rx}\pi \bar{D}_{t/rx}}{\sigma\pi d_{wt/rx}^{2}} \quad (1)$$

$$L_{t/rxa} = \mu_0 N_{t/rx}^{2} \frac{\pi \bar{D}_{t/rx}^{2}}{4l_{t/rx}} \quad (2)$$

respectively, where D_{tx} is the average transmitter coil

diameter and l_{tx} is the transmitter coil length. A cross section of the air-core receiver coil is also included in Fig. 2, where wire with diameter, d_{wrx} = 0.16 mm, was used to wind 232 turns over a length of 10 mm. Again, (1) and (2) were applied to predict values of resistance, R_{rxa}, and inductance, L_{rxa}, respectively and measurements were performed to confirm them.

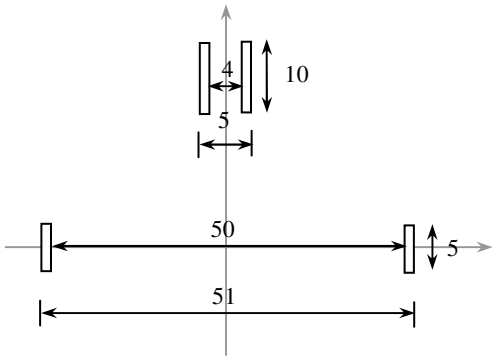

Fig. 2. Cross section of test transmitter and receiver coils. (Dimensions in mm, not to scale).

As shown in Table 1, measured resistance values are generally larger than predicted by, and this is explained by the additional length of wires needed to facilitate measurements. Equation (2) is more accurate for long thin coils like the receiver in this case than for flat (transmitter-like-) coils. Other formulas for inductance will be investigated in the final paper.

As the space available for accommodating a magnetic core in the receiver coil is very narrow, the range of suitable magnetic core materials is very limited. As a first step in this work, a strip of Vitrovac 6025X magnetic foil from Vacuumshemlze was applied, whose relative permeability is specified as large as 100,000 [8]. The foil was rolled to fit within the inner diameter of the receiver coil. Due to the non-uniform structure of the resulting core, a formula for inductance was not readily available and therefore it was necessary to measure the coil inductance as given in Table 1. Work is ongoing to identify other core materials that may be applied.

In order to complete the equivalent circuit model for the coils, each receiver coil was fixed concentrically at an axial distance of 5.5 cm from the transmitter coil, and the mutual inductance, M, was deduced. For the air-core coil, the equation [3]

$$M_a = \mu_0 \frac{\pi}{2l_{rx}} N_{tx} N_{rx} \frac{\overline{D}_{rx}^{\,2}}{4} \left(\frac{l_{rx}+l_{sep}}{\sqrt{\overline{D}_{tx}^{\,2}/4+(l_{rx}+l_{sep})^2}} - \frac{l_{sep}}{\sqrt{\overline{D}_{tx}^{\,2}/4+l_{sep}^{\,2}}} \right) \quad (3)$$

was found to provide good agreement with measurements, where a value of 39.1 nH was predicted. Measurement was difficult in this case as the receiver signal amplitude was comparable to noise signals. For the coil with a magnetic core, M_m was measured in terms of the open-circuit voltage induced on the receiver coil, V_m, for a given current, I_{tx}, flowing in the transmitter coil:

$$M_m = V_m / (\omega I_{tx}) \quad (4)$$

TABLE I
TEST COIL PARAMETERS

Impedance	Predicted	Measured
R_{tx}	0.14 Ω	0.2 Ω (DC)
L_{tx}	49.3 µH	10.7 µH (300 kHz)
R_{rxa}	1.25 Ω	4.3 Ω (DC)
L_{rxa}	85.0 µH	60.5 µH (300 kHz)
M_a	39.1 nH	40.9 nH (300 kHz)
R_{rxm}	1.25 Ω	4.3 Ω (DC)
L_{rxm}	na	388 µH (300 kHz)
M_m	na	181.7 nH

Formulas for cylindrical core shapes will be investigated in the future. As expected, M_m at 182 nH was much larger than M_a. The corresponding increase in power is illustrated in section IV.

III. RESONANT CIRCUIT DESIGN

Conditions for maximum power transfer between given transmitter and receiver coils are investigated in this section for both case of air and magnetic cores in the receiver. For that purpose, the dimensions and relative locations of the coupled coils are kept constant, and the circuit of Fig. 1 is optimised for a range of operating frequencies.

It is well known that a resonant capacitor enhances power transfer in loosely coupled inductive power systems, where the high impedance of the inductive coils would limit current levels produced otherwise. For a given set of coils and a defined voltage source (as shown in Fig. 1), resonance is considered first on the receiver side, where the resonant capacitor, C_{rx}, can be found simply as

$$C_{rx} = \frac{1}{(2\pi f_{res})^2 L_{rx}} \quad (5)$$

for a resonant frequency, f_{res}. Under no-load conditions, the effect of C_{rx} is to enhance the open-circuit voltage induced across the terminals of the receiver coil, V_m according to

$$\underset{\sim}{V}_{nl} = \frac{1}{1-\omega^2 L_{rx} C_{rx} + j\omega R C_{rx}} \underset{\sim}{V}_m \quad (6)$$

where at the resonant frequency, $\omega_{res} = 2\pi f_{res}$, the factor of enhancement is given by

$$\underset{\sim}{V}_{nl} = -j\frac{1}{R}\sqrt{\frac{L_{rx}}{C_{rx}}}\,\underset{\sim}{V}_m = -jQ_{rx}\,\underset{\sim}{V}_m \quad (7)$$

with $Q_{rx} = \omega_{res} L_{rx}/R_{rx}$. The corresponding level of power delivered to a load resistance, R_L, at resonance is found to be

$$P = \frac{V_L^{\,2}}{R_L}, \text{ with } \underset{\sim}{V}_L = \frac{R_L}{R_{rx} + j\omega_{res}(L_{rx} + R_L R_{rx} C_{rx})} \underset{\sim}{V}_m \quad (8)$$

where maximum power is given by

$$P_{max} = \frac{V_m^{\,2} Q_{rx}}{2R_{rx}\left(Q_{rx} + \sqrt{1+Q_{rx}^{\,2}}\right)} \quad (9)$$

with a 'matched' load resistance

$$R_{Lm} = \sqrt{\frac{L_{rx}}{C_{rx}}}\sqrt{1+\frac{L_{rx}}{R_{rx}^{\,2} C_{rx}}} = \sqrt{\frac{L_{rx}}{C_{rx}}}\sqrt{1+Q_{rx}^{\,2}} \quad (10)$$

For a given receiver coil, (9) and (10) define conditions for maximum power transfer in terms of the coil impedance,

resonant capacitance and open-circuit induced voltage, V_m, and may be applied to predict the variation in power with increasing frequency.

While values of L_{rx} and C_{rx} remain relatively constant in (9) and (10), the main issue in predicting values of R_{Lm} and P_{max} is the variation of R_{rx} with frequency. Three different methods for determining R_{rx} were applied in this work. For the air-core coil, R_{rx} was measured as series resistance using a 4395A Impedance Analyser from Agilent. In order to ensure that all loss components were included, the parallel combination of the air-core receiver coil and its resonant capacitor was also measured and R_{rx} was deduced as

$$R_{rx} = \frac{L_{rx}}{C_{rx}\sqrt{Z_{rx}^{\,2} - (1/\omega C_{rx})^2}} \tag{11}$$

at each value of resonance considered. Values from both methods are compared in Fig. 3.

Inclusion of a magnetic core in the receiver coil provided higher output voltage levels than for the air-coil under open-circuit and no-load conditions, and therefore it was possible to apply (7) to determine Q_{rxm} from voltage measurements. Corresponding values of R_{rxm} are included for comparison with R_{rxa} in Fig. 3.

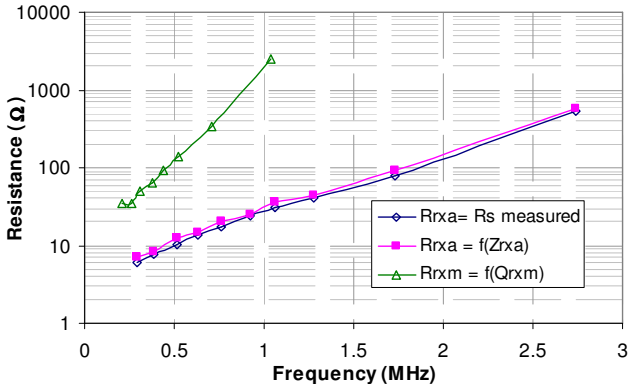

Fig. 3. Comparison of R_{rxa} and R_{rxm} measured using different methods.

Clearly, R_{rx} increases significantly with frequency for both coils, and this, along with coupling factor is the main factor that limits the output power of inductive power systems. There is generally agreement between both methods for measuring R_{rxa}, indicating that the contribution of losses from other circuit components is minimal. Due to losses in the core material, R_{rxm} is much higher than R_{rxa} at all frequencies. The corresponding effect on output power available is illustrated in section IV.

As given by (4), open-circuit voltage induced on the receiver coil, V_m, is directly proportional to current flowing in the transmitter coils, I_{tx}. In order to provide maximum current with a given source, resonant conditions must be applied at ω_{res}, where the effect of reflected impedance from the receiver circuit should be included. For a voltage of V_s with a source resistance, R_s, as applied in this case, current flowing in the transmitter coil, I_{tx}, is then calculated as

$$I_{tx} = \frac{V_s}{\sqrt{R_{tx}^{\,2} + \omega^2 (L_{tx} + R_{tx} R_s C_{tx})^2}} \tag{12}$$

and can be used to predict V_m and P_{max} according to (4) and (9), respectively. It is interesting to note that due to very low coupling levels in this case, the capacitor predicted by including reflected impedance was found to be very close to $C_{tx} = 1/(\omega_{res}^{\,2} L_{tx})$.

IV. Measurements

A. Air-core coils

The procedure described in section III was applied to design the inductive power system of Fig. 1 for the 232 turn air-core coil over a range of frequencies. Resonant capacitor values for the test frequencies are listed in Table II. No-load voltage waveforms measured across the transmitter coil and at the load terminals are presented at 294 kHz in Fig. 4, while the corresponding power level vs. frequency is plotted in Fig. 5.

TABLE II
Resonant Capacitance vs. Frequency

Frequency (kHz)	C_{rx} (nF)	C_{tx} (nF)
1064	0.33	2.0
924	0.47	2.8
764	0.68	4.0
634	1.00	5.8
514	1.50	8.5
384	2.70	15.2
294	4.70	27.0

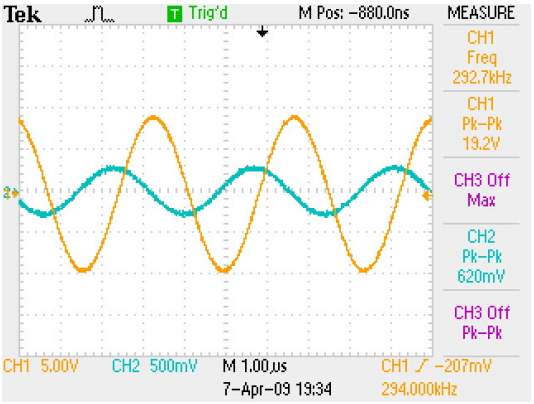

Fig. 4. Voltage waveforms measured across transmitter coil (CH1) and load terminals (CH2) at 294 kHz (R_{Lm} = 2.9 kΩ).

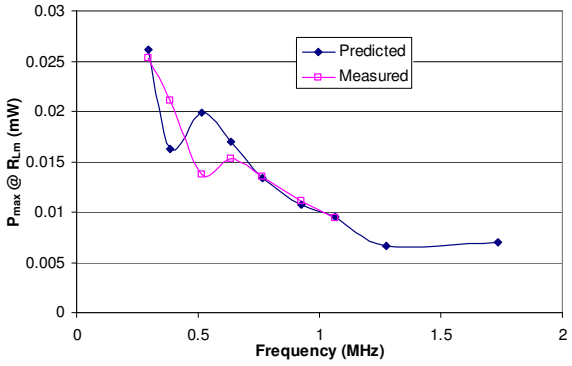

Fig. 5. Measured power vs. frequency for air-core coils

B. *Coils with a magnetic core*

A similar procedure was applied to determine maximum power levels available when the magnetic core is included in the receiver coils. Measured transmitter and receiver voltages for the load that provides maximum power at 210 kHz are plotted in Fig. 6, while maximum power vs. frequency for the coils is plotted in Fig. 7.

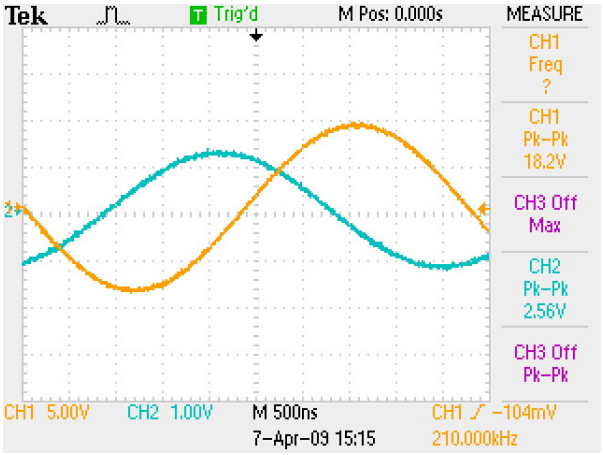

Fig. 6. Voltage waveforms measured across transmitter coil (CH1) and load terminals (CH2) at 260 kHz (R_{Lm} = 7.5 kΩ).

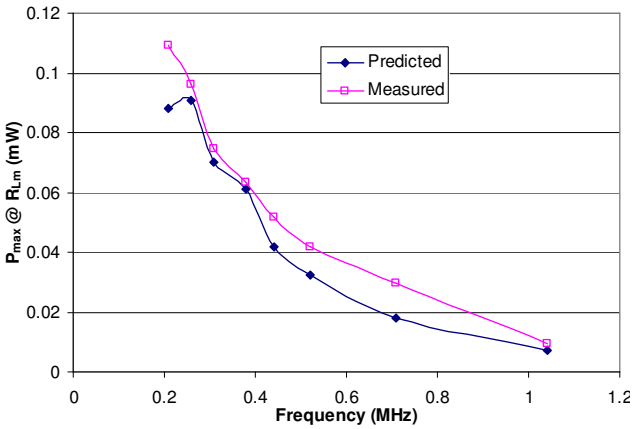

Fig. 7. Power vs. frequency for coils with a magnetic core

C. *Analysis*

For both cases of air-core and magnetic core, it is seen that there is good agreement between modelled and measured values of power. Voltage and power levels achieved with the magnetic core are approximately four times larger than equivalent air-core values.

The decrease in power with increasing frequency is explained by reducing current on the transmitter side, I_{tx}, as the impedance of each coil increases. In a biomedical application, I_{tx} will be limited by the maximum magnetic field intensity that can be applied. Therefore, in order to normalize the results in terms of I_{tx}, results of power are compared for both coils in Fig. 8 at the maximum current level allowed according to standards for safe H-field exposure levels for humans [9]. As shown, higher power levels are achieved when a magnetic core is included than with the same air-core coils. Higher power is achieved at lower frequency because of smaller values of R_{rx} which contribute to increasing the loaded Q_{rx} and consequently the power transfer capability.

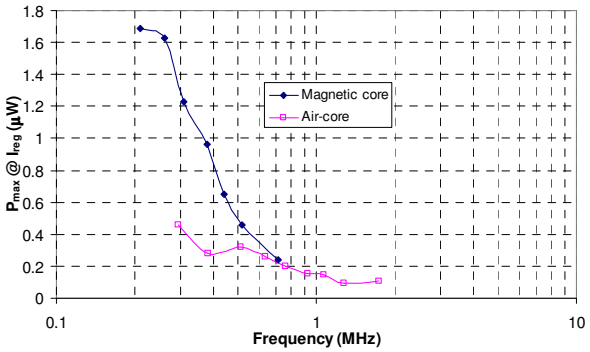

Fig. 8. Power at biomedical field limits vs. frequency for air and magnetic-core receiver coils

V. Conclusions and Future Work

Models and measurement results illustrate how the performance of magnetic materials can enhance power levels within a given system. However, power levels are shown to be similar for equal transmitter currents. Future work will investigate the performance of different magnetic core materials, in addition to considering the implications of a battery power source and biomedical field limits.

Acknowledgment

The authors wish to acknowledge the support of Vacuumschmelze in providing a sample of Vitrovac 6025X for testing.

References

[1] Lenaerts B; Puers, R; 'Omnidirectional Inductive Powering for Biomedical Implants (Analog Circuits and Signal Processing)', Springer, October 24, 2008

[2] Zierhofer, C.M.; Hochmair, E.S.; 'Geometric approach for coupling enhancement of magnetically coupled coils', *IEEE Transactions on Biomedical Engineering*,Vol. 43, Issue 7, July 1996, Page(s):708–714

[3] Pichorim, S.F.; Abatti, P.J.; 'Design of coils for millimeter- and submillimeter-sized biotelemetry', *IEEE Transactions on Biomedical Engineering*, Volume 51, Issue 8, Aug. 2004 Page(s):1487 - 1489

[4] Harrison, R.R.; 'Designing Efficient Inductive Power Links for Implantable Devices' IEEE International Symposium on Circuits and Systems, 2007. ISCAS 2007, 27-30 May 2007, Page(s):2080 - 2083

[5] Schulman, J.H.; Mobley, J.P.; Wolfe et al.; 'Battery powered BION FES network' *26th Annual International Conference of the IEEE Engineering in Medicine and Biology Society*, 2004. IEMBS '04. Volume 2, 1-5 Sept. 2004 Page(s):4283 - 4286

[6] Hmida, G. B.; Ghariani H.; Samet, M;, 'Design of wireless power and data transmission circuits for implantable biomicrosystem', *Biotechnology*, 6 (2): 153 – 164, 2007

[7] Kendir, G.A. et al.; 'Efficient inductive power link design for retinal prosthesis', *Proceedings of the 2004 International Symposium on Circuits and Systems, 2004,* ISCAS '04, Volume 4, 23-26 May 2004 Page(s):IV - 41-4 Vol.4

[8] Vacuumschmelze, 'Soft Magnetic Materials and Semi-finished Products', http://www.vacuumschmelze.de

[9] IEEE, Piscataway, NJ, 'Standard for safety levels with respect to human exposure to radio frequency electromagnetic fields, 3 kHz to 300 GHz', *IEEE Std. C95.1.*